

Dose optimization of abdominal CT protocols: Implementation of a task-based approach to the national diagnostic reference levels in Switzerland

PI: Prof. Sebastian Schindera (KSA), co-PI: Prof. Francis R. Verdun (CHUV)
Medical physicists involved: Dr Christoph Aberle (USB), Dr Damien Racine –Dr Anaïs Viry (CHUV), Dr Thiago V.M. Lima (KSA)

Final report, November 2019

Notice

The results presented in this document should not be used without a prior written agreement from the PI of the project.

Introduction

The purpose of this work is to investigate a way to propose a framework for patient dose optimization of abdominal CT that not only considers the dose aspect but also the image quality aspect.

For many years, the focus in radiation protection to optimize clinical protocols was to ensure some kind of compliance with national diagnostic reference levels (DRL) without paying that much attention to image quality. This comes from the fact that the parameters used to assess image quality were too far from the actual radiological needs. The introduction of iterative reconstruction has required changing paradigm since the use of the technical parameters for assessing image quality could not be applied straightforwardly. A better approach is to express image quality in terms of essential tasks that have to be done by the radiologists to answer clinical questions. The first basic task is the detection of pathological structures; a task that is in fact a classification task (signal present/signal absent). Other tasks can then be defined to perform estimations (such as lesion density, shape, volume measurements).

The goal of this project is to focus on the task of structures detection in abdominal CT for three common clinical protocols: renal stone detection, appendicitis or diverticulitis and search for focal lesions in the liver.

Material and methods

Description of CT

Table 1 summarizes the CT units involved in the study

CT	Algorithm
GE	
BrightSpeed S	ASIR 50 (ASIR 50% (SS50 Slice 50%), recon mode "Full", Convolution Kernel "Soft")
HD 750	ASIR-V 50 (ASIR-V 50% (AR50 Slice 50%), recon mode "Full", Convolution Kernel "Standard")
Revolution	ASIR-V 50 (ASIR-V 50% (AR50 Slice 50%), recon mode "Full", Convolution Kernel "Standard")
Philips	
Brilliance 16	FBP (filter: Standard (B), enhancement: 0.0)
Ingenuity	iDose⁴ level 3 (out of 6), filter: Standard (B), enhancement 0.0, adaptive filter: yes
Brilliance iCT	iDose level 3 (out of 6), filter: Standard (B), enhancement 0.0, adaptive filter: yes
Siemens	
Somatom Emotion 16	FBP (kernel: b30s)
Somatom Definition Edge	ADMIRE 3 (kernel: i30s)
Somatom Force	ADMIRE 3 (kernel: Bf40s)
Toshiba / Canon	
Aquilion RXL	AIDR 3D Standard , Filter: OFF, ReconFC: FC18, Boost: OFF, Interp TCOT+, F/H: -
Aquilion CXL	AIDR 3D Standard , Filter: OFF, ReconFC: FC18, Boost: OFF, Interp TCOT+, F/H: -
Aquilion ONE Vision Edition	AIDR 3D enhanced Standard , Filter: OFF, ReconFC: FC08, Boost: OFF, OSR: ON (Body), Interp V-TCOT, F/H: -

Table 1: CT scanners involved in the present study

The acquisitions will be performed with automatic tube current modulation, ATCM, and reconstruction will be done with iterative reconstruction (if available).

High contrast detectability: Description of the phantom and the image quality metrics

Iterative Reconstruction algorithms are known to be highly non-linear and non-stationary which introduces a dependency of image contrast and noise on the spatial resolution [1-3]. To take into account this dependency the target transfer function (TTF) metric was used to characterize the spatial resolution as advised by most of the groups working in the field of image quality assessment in CT.

For this project, a semi anthropomorphic abdomen phantom with medium annulus (QRM, Moehrendorf, Germany) that represents the attenuation of an abdomen of a standard adult was used to assess the low contrast detectability. The phantom is composed with materials tissue equivalents that mimics muscle, liver, spleen and bone (vertebrae).

It contains a module with a cylindrical lesion with a contrast of 200 HU relative to background (\varnothing 20 mm) (see Figure 1 left). The cylindrical lesion was used to calculate the TTF and contrast parameter and the homogeneous part of the module (see Figure 1 right) allowed the assessment of the Noise Power Spectrum (NPS), (extensive details and explanations on the methodology can be found in the paper of Verdun and Racine et al. [4]).

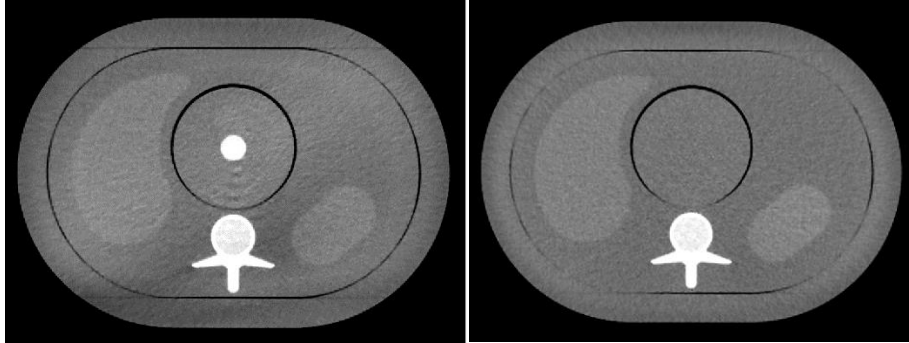


Figure 1: From left to right: Picture of the phantom used to assess the spatial resolution characteristics and the homogeneous part used to assess the image noise parameter

The contrast, TTFs and NPS metrics were used to compute the detectability index (d') of a 3-mm-diameter structure having contrast values of 350 HU with a NPWE model observer.

$$d' = \frac{\sqrt{2\pi} \Delta HU \int_0^{f_{Ny}} S^2(f) TTF^2(f) VTF^2(f) f df}{\sqrt{\int_0^{f_{Ny}} S^2(f) TTF^2(f) NPS(f) VTF^4(f) f df}}$$

Where, $VTF(f)$ is the visual transfer function of the human eye $VTF(f) = f^{1.8} \exp(-0.6f^2)$ and $S(f)$ the Fourier transform of the simulated object (i.e. spherical structure with a diameter of 3 mm) and f_{Ny} is the Nyquist frequency[3].

Low contrast detectability: Description of phantom and image quality metrics

The same semi anthropomorphic abdomen phantom, but with another module was used to assess the low contrast detectability. This module contains spherical lesions with a contrast of -20 HU relative to background (in particular \emptyset 8.0 mm for diverticulitis and 5.0 mm for focal liver lesion).

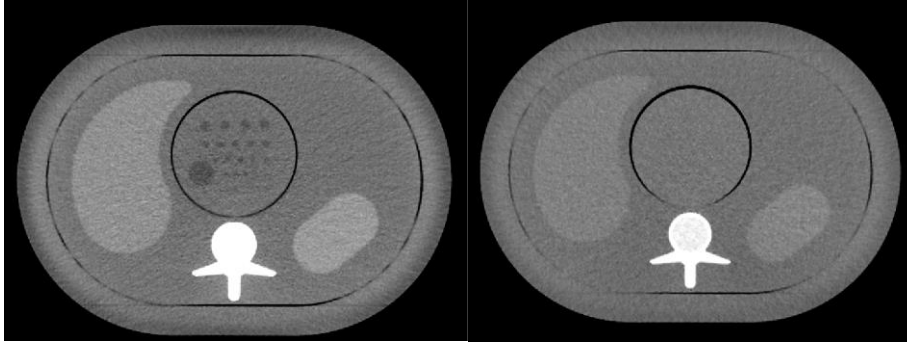


Figure 2: From left to right: Part of the phantom used to extract signal and the homogeneous part of the phantom used to extract the noise in the image

In this study, we have chosen a linear anthropomorphic Channelized Hotelling (CHO) model observer that is well known to mimics human observers detection performance. Model observers are mathematical models based on the statistical decision theory. With a linear observer model, the decision variable λ is given by the dot product between the template \mathbf{w} and the channels output \mathbf{v} . (extensive details and explanations on the methodology can be found in the paper of Verdun and Racine et al. [4], and in Racine et al. [5]).

$$\lambda_{\text{CHO}} = \mathbf{w}_{\text{CHO}}^T \mathbf{v}$$

These channelized models take advantage of the spatial selectivity behavior of the human visual system. With the adopted notation, a channel is a $N \times 1$ column vector that produces a scalar output when multiplied by the image \mathbf{g} . The ensemble of the J channels can therefore be written as an $N \times J$ matrix where each column is one of channel \mathbf{u}_j .)

$$U = [\mathbf{u}_1, \mathbf{u}_2, \dots, \mathbf{u}_J]$$

The channel output \mathbf{v}_i is obtained by the dot product between the channel \mathbf{u}_j and the image \mathbf{g} .

$$\mathbf{v}_i = \mathbf{u}_j \mathbf{g}$$

The template of the resulting covariance matrix is calculated from the images containing no signal.

$$\mathbf{w}_{\text{CHO}} = (\mathbf{K}_{\mathbf{v}/\mathbf{n}})^{-1} \langle \mathbf{v}_s - \mathbf{v}_n \rangle$$

where $\mathbf{K}_{\mathbf{v}/\mathbf{n}}$ represents the covariance matrix computed from channelized images containing no signal, $\langle \mathbf{v}_s \rangle$ represents the mean vector containing the data of the signal images as seen through the channels, and $\langle \mathbf{v}_n \rangle$ represents the mean vector containing the data of the signal-absent images as seen through the channels.

Difference of dense Gaussian channels, D-DoG

In this study, the target to be detected is of spherical symmetry. In such a case, the channels recognized, as a good approximation of human vision is the dense of difference of Gaussian (D-DoG) which allows the use of a limited number of channels. This is particularly important since the more channels to be used the more images need to be produced (as a rule of thumb a total of at least J^2 images; J being the number of channels). In our situation, it is

admitted that 10 channels are sufficient to produce sound results. The radial profile of each frequency of the D-DoG is given by the following formula:

$$C_j(\rho) = e^{-\frac{1}{2}\left(\frac{\rho}{Q\sigma_j}\right)^2} - e^{-\frac{1}{2}\left(\frac{\rho}{\sigma_j}\right)^2}$$

where ρ is the spatial frequency, j the channel number, Q the bandwidth of the channel and, σ_j the standard deviation of each channel. Each σ_j values is given by $\sigma_j = \sigma_0 \alpha^{j-1}$. Factor Q is the bandwidth of the filter. Generally the parameters used are: $\sigma_0 = 0.005$, $\alpha = 1.4$ and $Q = 1.67$ [6].

Model observers like CHO with well-suited channels are more efficient than human observers, for simple detection tasks such as Signal Known Exactly / Background Known Exactly (SKE/BKE). To adjust the detection outcomes of model observers to human observers it is necessary to add some internal noise. The model used in this project is equivalent to injecting internal noise with covariance matrix proportional to the external-noise covariance matrix as it is often made with such a problematic [7]:

$$K_{v/n} = K_{int} + K_{ext} \quad \text{Where } p \text{ is the the weighting factor and } [K_{int}]_{i,i} = p \cdot [K_{ext}]_{i,i}$$

A Dose Efficiency Index (DEI)

The abdominal QRM phantom with its module was scanned at five dose levels (4, 8, 12, 16 and 20 mGy) on the different CT units (Table 1) using the Appendicitis or diverticulitis protocols. The CHO with DDoG channel was used to compute an AUC (area under the ROC curve).

Finally, a comparison of the performances of the different units will be provided allowing to estimate the variation of image quality in terms of dose when changing CT unit. We proposed an analysis of the data with the proposal of a strategy to establish a dose efficiency index (DEI) to quantify the CT unit performances in terms of low contrast detectability assessment for different fixed dose levels. A Dose Efficiency Index (DEI) will be introduced to classify the CT scanners in terms of image quality performance. The DEI is defined by the integral of the area under the curve image quality (AUC) as a function of dose.

CTDI_{vol} assessment

Before each acquisition session, the CTDI_w was measured and compared to the CTDI_w displayed. Then difference calculated between both CTDI_w was used to correct with a specific factor the CTDI_{vol} displayed for the acquisitions. In all results, the CTDI_{vol} used was the corrected CTDI_{vol}.

Acquisition

Images have been acquired using six successive scans of the phantom using renal stones protocols (without any phantom position change) allowing 78 images to calculate the TTF and contrast, and 96 images to calculate the NPS. For the Appendicitis protocols or focal liver lesion protocols phantom has been scanned twenty times, without any phantom position change, allowing 80 ROI to be obtained with the targets, and 900 ROI without any target. To ensure that imaging characteristics were comparable when dealing with images with or without target scanning, a similar homogeneous modulus (containing no contrast) was scanned in similar conditions (the same position within the phantom was thus considered).

	CTDI_{vol} (mGy)
Renal stones protocol	15
	10
	6
	4
	2
Appendicitis protocols and focal liver lesion protocols	20
	16
	12
	8
	4

Table 2: CTDI_{vol} used with the different protocols

The dose range proposed to investigate the image quality parameter that characterizes this protocol was the result of the survey organized in 2016-2017 to update the Swiss DRL values [8]. The different dose values used in this project are summarized in Table 2. The main acquisition and reconstruction parameters are described in the Annex: data acquisition protocols.

Results

To ensure impartiality of this work the results will be reported in an anonymous manner; since the goal is to demonstrate the feasibility and potential of the methodology, rather than to evaluate specifically the selected units. The list used is given in the Table 1 where the year of introduction is mentioned.

CTDI_{vol} assessment

The difference between the CTDI_w displayed and the CTDI_w measured was smaller than 5 % for all CT except for the GE BrightSpeed S, the Philips Brilliance 16 and the Philips Brilliance iCT. For these two units the CTDI_{vol} displayed was corrected by a correction factor of 0.86, 0.91 and 0.85, respectively. CTDI_{vol} was evaluated at the position of the lesions if the tube current was modulated.

Internal noise calibration

From data used for the study “Inter-laboratory comparison of Channelized Hotelling Observer computation”, Ba et al. it appears that “p” factor set to 20.1 provided a good match between the CHO and human observers. We decided to take that “p” factor to evaluate the image quality with the CHO model in this study.

A Dose Efficiency Index to benchmark CT concerning the low contrast resolution

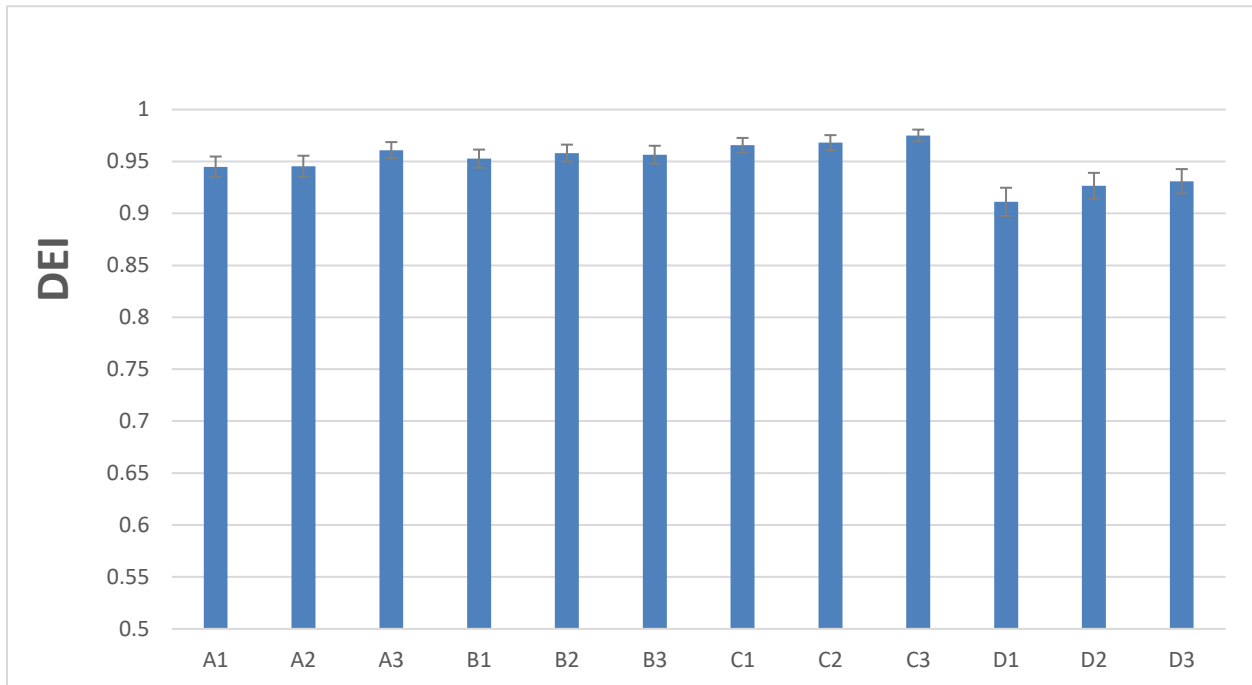


Figure 3: Characterization of clinical CT systems using a DEI

The best DEI is obtained with C3 CT scanner whereas the lowest DEI is obtained with D1 CT scanner. In spite of the small differences obtained for the DEI, the differences are statistically significant.

Renal stone protocols

As expected, the image quality assessed in term of a detectability index increased with the dose for the different CTs. Comparing the manufacturers included in this study it appears that the detectability index reached the highest score for Siemens. However, in terms of AUC, when dealing with the present DRL dose level (CTDI_{vol} equals to 6 mGy) for this clinical question, the CT technologies variation has no impact on the detection of renal stones since a

detectability index greater than 10.0 already allows a 100% detection (Figure 3). It means when the dose varied, the performance was always maximal whatever the dose level even at 2 mGy. Nevertheless, dose might have an impact on the shape, size and CT number precision (it will be investigated in the future). Thus, for actual quantitative measurements 2 mGy might be insufficient.

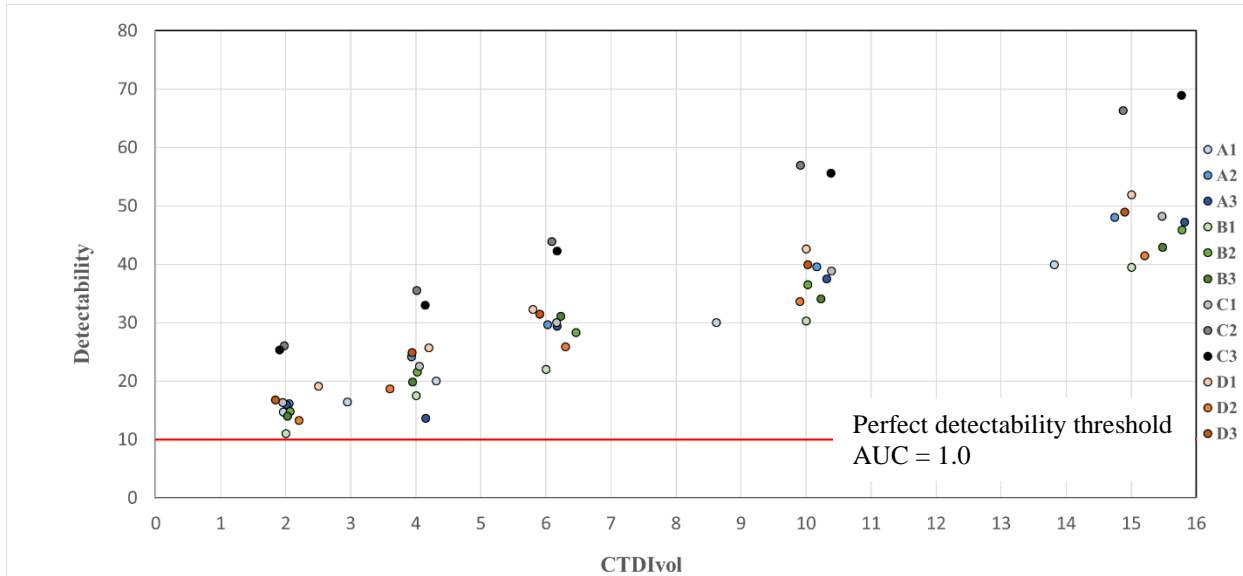


Figure 4: Detectability index of the 3mm/450 HU target as a function of dose for the different CT systems

A linear relationship between the logarithm of the dose indicator and the logarithm of the detectability index was found for every CT. It is thus possible to extrapolate data to find at which dose level the detectability decreases (AUC < 1.0). The AUC is inferior to 1.0 when the CTDIvol is inferior to 2 mGy.

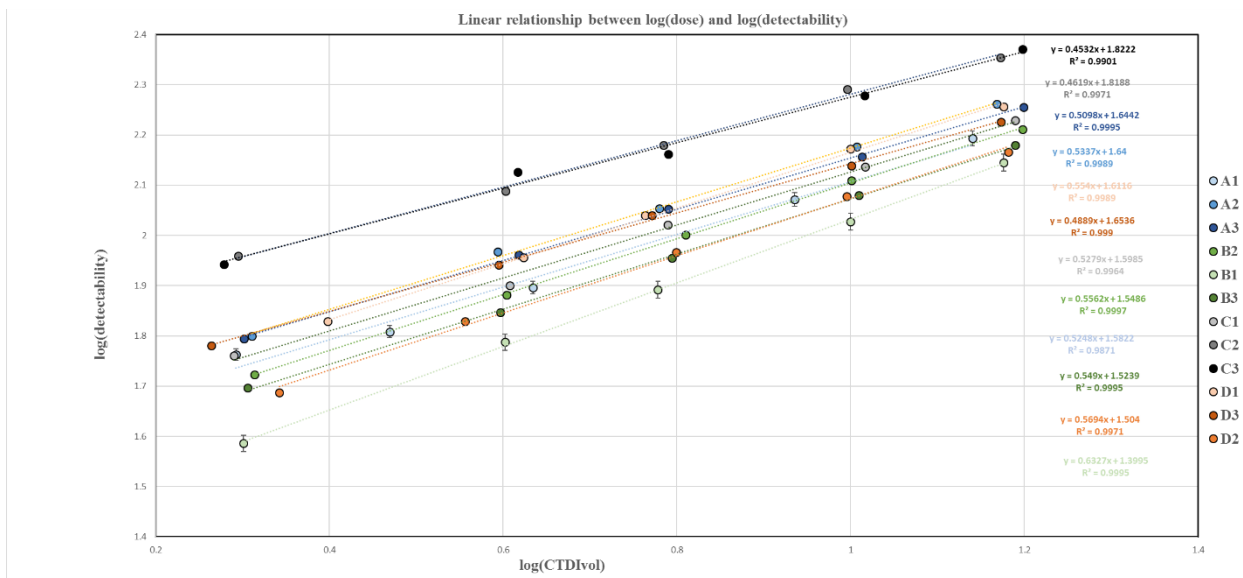


Figure 5: Log(Detectability index) of the 3mm/450 HU target as a function of log(dose) for the different CT systems.

Appendicitis or diverticulitis

The results for the 8.0mm/20HU targets are summarized in Figure 5. As expected, the detectability index increased with the dose for all CTs. Moreover, imaging the medium abdomen phantom with a CTDI_{vol} of 15 mGy or higher (see Figure 5) had no major difference on the outcome whatever the scanner used.

Reducing the CTDI_{vol} to 11 mGy or lower (DRL proposed in 2018 for abdomen protocols), the image quality metrics decreased for all scanners (Mean AUC being lower than 0.95) with a larger reduction observed for Canon manufacturer. At the lowest CTDI_{vol} we investigated (4mGy), only Siemens Force scanner provided better results than other ones.

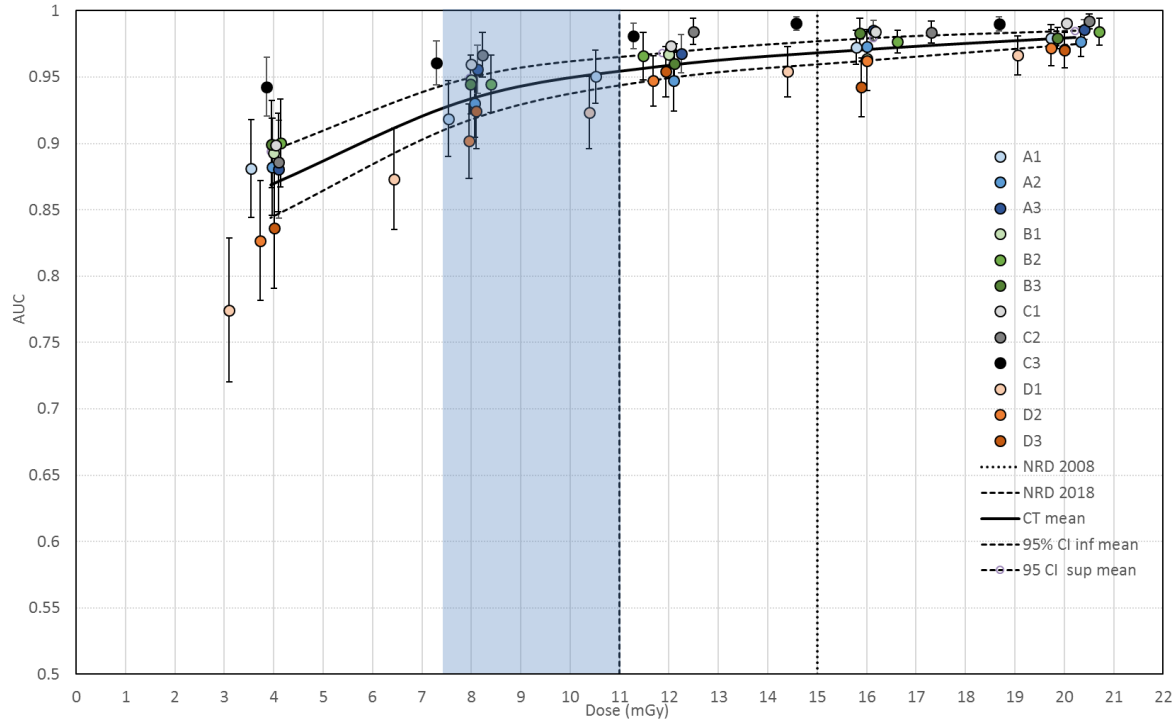


Figure 6: Area under the curve (AUC) of the 8mm/20 HU targets as a function of dose for the various CT systems. The blue area represented the P25 – P75 range of the abdominal DRL

Search for focal lesion in the liver protocols

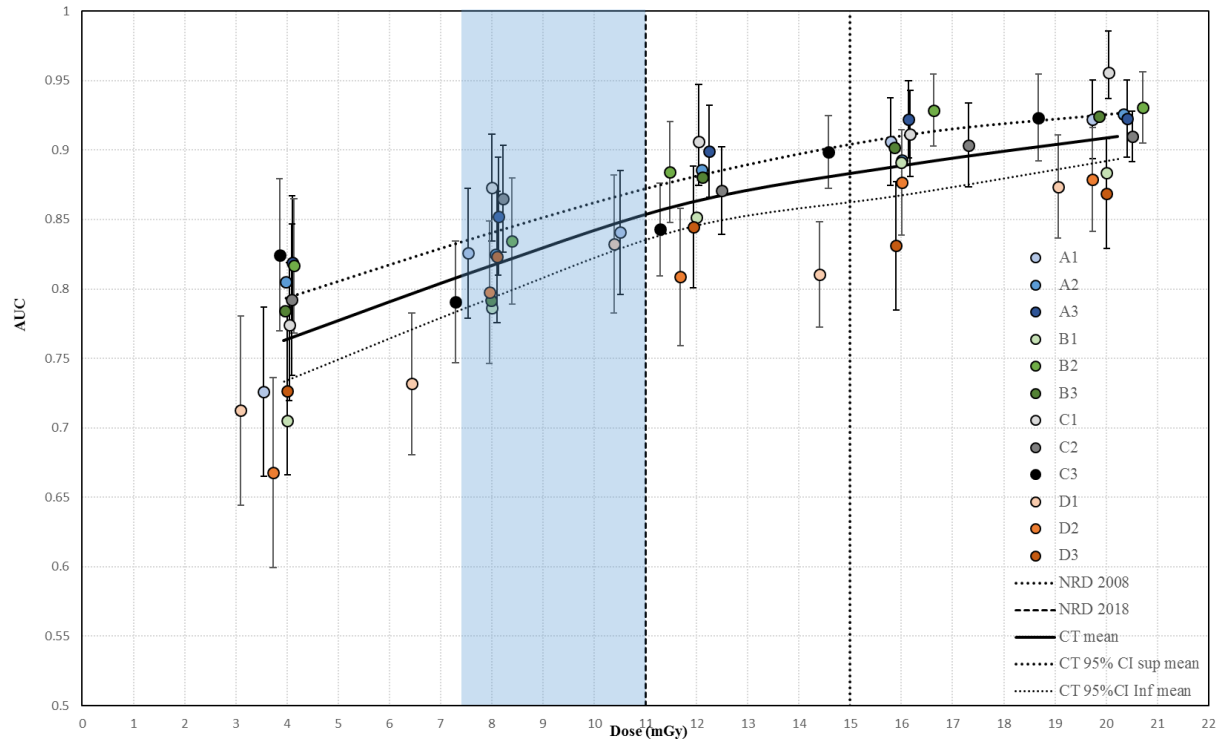


Figure 7: Area under the curve (AUC) of the 5mm/20 HU targets as a function of dose for the various CT systems. The blue area represented the P25 – P75 range of the liver DRL

Searching focal liver lesion is a more difficult task than the two previous clinical task presented. It was thus proposed to focus on a smaller lesion (5.0 mm instead of 8.0 mm) with a similar contrast level (20 HU). As expected with such a difficult task a large variability in image quality especially when dealing with low dose appears. In addition, even at a high dose level (superior to 20 mGy), the image quality did not reach a plateau.

Search the minimum AUC required for clinical indication

Using different dose levels it is possible to reach a similar level of image quality for all scanners (differences within 5%). However, as expected from the DEI results this comparable level of image quality is obtained at noticeable different $CTDI_{vol}$ values. For example for appendicitis or diverticulitis protocol the same image quality (AUC = 0.95) can be obtained with a range of dose between 8.0 and 12.0 mGy. For the focal liver lesion protocol, the range is 9 – 12.5 mGy to obtain the same AUC (equal to 0.85). This should initiate a discussion among the radiologists community to set the minimum AUC required depending the clinical indications for a safe diagnosis. It should be kept in mind that with a simple phantom as the one used here the minimum, an AUC of 0.9 to detect correctly focal liver lesion requires a range of dose of 15 to 21 mGy. This is of particular importance for that particular case since the use of a $CTDI_{vol}$ of 11 mGy, corresponding to the DRL of that anatomical region and where 75% use a lower value, lead to a range of AUC between 0.835 and 0.875 (95 % C.I.=5%), and between 0.785 and 0.845 for a $CTDI_{vol}$ of 7.5 mGy (P25 of the DRL).

Discussion - Conclusion

In the framework of patient dose optimization, it is essential to ensure that comparable task-based image quality levels are obtained. A full characterization of image quality in CT units would require assessment of a large number of parameters such as the acquisition time, the standard high and low contrast resolutions, the temporal resolution, the energy resolution when dealing with kV optimization or dual energy imaging, impact of patient morphology etc...

According to this report, the low and high contrast detection have been evaluated on specific conditions on twelve different CT scanners.

The results obtained show that it is possible to compare units using several task-based paradigms, and thus ensure a comparable level of image quality for several types of CT units used in clinical routine one can require significant dose different to reach the same outcome when dealing with the low contrast detectability. In addition, the present DRL for liver CT examinations might be too low when dealing with the detection of subtle lesions.

Perspectives

The outcome of this project leads to very interesting results that are worth publishing in a European journal of radiology. The methodology presented has some limitations such as the use of a homogeneous background. However, even with such a simplified paradigm it has been possible to show the limit of applying the DRL concept without taking into account the image quality parameter. One possible way to ensure an adequate image quality level across Switzerland could be the application the presented methodology at national level. The SSR/SGR and SSRMP could promote this action. It could be, for example, interesting to use this kind of approach during the auditing process. Finally, this study could be continued by using realistic backgrounds and lesions to be detected still using model observers.

Scientific presentations

Dose optimization of abdominal CT protocols: Implementation of a task-based approach to assess image quality in relation to the national diagnostic reference level in Switzerland

D. Racine, A. Viry, C. Aberle, F. R. Verdun, R. Treier, S. T. Schindera

Swiss Congress of Radiology 2019

Saint Gall, Suisse, 13-14 juin 2019

(Oral presentation)

Evaluation of the image quality on abdominal CT protocols based on Swiss diagnostic reference levels

D. Racine, A. Viry, C. Aberle, T. Lima, F. R. Verdun, R. Treier, S. T. Schindera

Optimisation in X-ray and Molecular Imaging 2020

Gothenburg, Sweden, 20-22 April 2020

(Abstract submitted)

Reference

- [1] Richard S, Husarik D B, Yadava G, Murphy S N and Samei E 2012 Towards task-based assessment of CT performance: System and object MTF across different reconstruction algorithms *Med. Phys.* 39 4115-22
- [2] Brunner C C and Kyprianou I S 2013 Material-specific transfer function model and SNR in CT *Phys. Med. Biol.* 587447-61
- [3] Ott JG, Becce F, Monnin P, Schmidt S, Bochud FO and Verdun FR An update on the non-prewhitening model observer in computed tomography for the assessment of the adaptive statistical and model-based iterative reconstruction algorithms. *Phys. Med. Biol.* 2014; 59:4047-4064
- [4] F.R. Verdun, D. Racine, J.G. Ott, M.J. Tapiovaara, P. Toroi, F.O. Bochud, W.J.H. Veldkamp, A. Schegerer, R.W. Bouwman, I Hernandez Giron, N.W. Marshall, S. Edyvean. Image quality in CT: from physical measurements to model observers. *Phys Med.* 2015 Dec;31(8):823-43. doi: 10.1016/j.ejmp.2015.08.007. Epub 2015 Oct 12. Review.
- [5] Racine D, Ba AH, Ott JG, Bochud FO, Verdun FR. Objective assessment of low contrast detectability in computed tomography with Channelized Hotelling Observer. *Phys Med.* 2016 Jan;32(1):76-83. doi: 10.1016/j.ejmp
- [6] Abbey CK, Barrett HH. Human- and model-observer performance in ramp-spectrum noise: effects of regularization and object variability. *J Opt Soc Am* 2001;18:473–88.
- [7] Brankov JG. Evaluation of the channelized Hotelling observer with an internal-noise model in a train-test paradigm for cardiac SPECT defect detection. *Phys Med Biol.* 2013;58(20):7159–7182. doi:10.1088/0031-9155/58/20/7159
- [8] Aberle C, Ryckx N, Treier R, Schindera S. Update of national diagnostic reference levels for adult CT in Switzerland and assessment of radiation dose reduction since 2010. *Eur Radiol* (2019). <https://doi.org/10.1007/s00330-019-06485-1>

Annex: data acquisition protocols

Renal stone protocols

High voltage	120 kV
Rotation time	0.8 s
X-ray collimation	40 mm
Kernel	Standard body filter
Reconstructed slice thickness	2.5 or 3 mm
Interval slice thickness	1.25 or 1.5 mm
CTDI with ATCM	Tune the ATCM settings to obtain a CTDI _{vol} equal to 2, 4, 6, 10, 15 mGy (phantom M)
Helical pitch	1
Reconstructed FOV	close to 37 cm
Phantom	QRM abdomen with annulus M with Calcium module
Series	6 repetitions

Appendicitis or diverticulis protocols

High voltage	120 kV
Rotation time	0.8 s
X-ray collimation	40 mm
Kernel	Standard body filter
Reconstructed slice thickness	2.5 or 3 mm
Interval slice thickness	1.25 or 1.5 mm
CTDI with ATCM	Tune the ATCM settings to obtain a CTDI _{vol} equal to 4, 8, 12, 16, 20 mGy
Helical pitch	1.3
Reconstructed FOV	close to 37 cm
Phantom	QRM abdomen with annulus and low contrast module
Series	20 repetitions

Focal liver lesion protocols

High voltage	120 kV
Rotation time	0.8 s
X-ray collimation	40 mm
Kernel	Standard body filter
Reconstructed slice thickness	2.5 or 3 mm
Interval slice thickness	1.25 or 1.5 mm
CTDI with ATCM	Tune the ATCM settings to obtain a CTDI _{vol} equal to 4, 8, 12, 16, 20 mGy (phantom M)
Helical pitch	1.3
Reconstructed FOV	close to 37 cm
Phantom	QRM abdomen with annulus and low contrast module